

# Branched Amphiphilic Cationic Oligopeptides Form Peptiplexes with DNA: A Study of Their Biophysical Properties and Transfection Efficiency

L. Adriana Avila,<sup>†</sup> Luana R. M. M. Aps,<sup>‡</sup> Pinakin Sukthankar,<sup>†</sup> Nicoleta Ploscariu,<sup>§</sup> Sushanth Gudlur,<sup>†</sup> Ladislav Šimo,<sup>||</sup> Robert Szoszkiewicz,<sup>§</sup> Yoonseong Park,<sup>||</sup> Stella Y. Lee,<sup>⊥</sup> Takeo Iwamoto,<sup>#</sup> Luis C. S. Ferreira,<sup>‡</sup> and John M. Tomich<sup>\*,†</sup>

<sup>†</sup>Department of Biochemistry & Molecular Biophysics, Kansas State University, Manhattan, Kansas 66506-3902, United States

<sup>‡</sup>Institute of Biomedical Sciences, University of São Paulo, São Paulo, São Paulo 05508-900, Brazil

<sup>§</sup>Department of Physics, Kansas State University, Manhattan, Kansas 66506-2601, United States

<sup>||</sup>Department of Entomology, Kansas State University, Manhattan, Kansas 66506-4004, United States

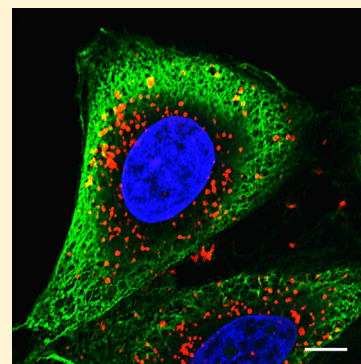
<sup>⊥</sup>Division of Biology, Kansas State University, Manhattan, Kansas 66506-3902, United States

<sup>#</sup>Division of Biochemistry, Core Research Facilities, Jikei University School of Medicine, Tokyo 105-8461, Japan

## Supporting Information

**ABSTRACT:** Over the past decade, peptides have emerged as a new family of potential carriers in gene therapy. Peptides are easy to synthesize and quite stable. Additionally, sequences shared by the host proteome are not expected to be immunogenic or trigger inflammatory responses, which are commonly observed with viral approaches. We recently reported on a new class of branched amphiphilic peptide capsules (BAPCs) that self-assemble into extremely stable nanospheres. These capsules are capable of retaining and delivering alpha-emitting radionuclides to cells. Here we report that, in the presence of double stranded plasmid DNA, BAPCs are unable to form. Instead, depending of the peptide/DNA ratios, the peptides either coat the plasmid surface forming nanofibers (high peptide to DNA ratio) or condense the plasmid into nanometer-sized compacted structures (at low peptide to DNA ratios). Different gene delivery efficiencies are observed for the two types of assemblies. The compacted nanometer-sized structures display much higher transfection efficiencies in HeLa cells. This level of transfection is greater than that observed for a lipid-based reagent when the total number of viable transfected cells is taken into account.

**KEYWORDS:** cationic branched peptides, BAPCs, nanofibers, condensed DNA, peptiplex, plasmid DNA, nonviral, gene delivery, nontoxic



## INTRODUCTION

The ability to deliver bioactive macromolecules into specific cell organelles holds the promise of treating a broad range of human diseases.<sup>1</sup> The first steps required for targeting subcellular organelles involve traversing the plasma membrane and then gaining access to the cytosol. Macromolecules such as plasmid DNA (pDNA) are anionic and show greatly reduced membrane bilayer permeability.<sup>2</sup> Typically they need to be associated with molecular carriers to facilitate their translocation into the cell.

A wide range of molecular carriers are currently available for pDNA delivery *in vitro*. Reports are emerging with increasing frequency describing modified or completely new transfection materials. Improvements in genome editing systems, such as CRISPR/Cas9 and zinc-finger nuclease (ZFN), have greatly improved integration of corrective sequences by making them site specific.<sup>3,4</sup> In addition to CRISPR/Cas9 and ZFN, peptide nucleic acid (PNA) molecules can be used to target specific

genes, inhibiting both transcription and translation, therefore showing potential application in antigene and antisense therapies.<sup>5</sup> Adding those types of genome editing elements has moved *nonviral gene delivery* closer to clinical applications.

Lipoplexes<sup>6</sup> (cationic lipid–DNA complexes) and polyplexes<sup>7</sup> (cationic polymer–DNA complexes) are examples of nonviral gene delivery systems.<sup>8–10</sup> Lipoplexes constitute self-assembling nanosystems formed as a consequence of the interaction of branched cationic lipids with the negatively charged DNA molecules to form complexes, with the cationic lipids encasing the dsDNA.<sup>11,12</sup> The most common structures for lipoplexes are the lamellar ( $L_{\alpha}$ ) phase with alternating lipid bilayer and DNA monolayers and inverted hexagonal ( $H_{II}$ )

**Received:** August 1, 2014

**Revised:** January 4, 2015

**Accepted:** February 3, 2015

**Published:** February 3, 2015

phase consisting of DNA coated with a lipid monolayer in a hexagonal lattice.<sup>13</sup> It has been argued that the H<sub>II</sub> phase complexes have a much higher transfection activity than the L<sub>α</sub> phase ones. One explanation could be that this phase promotes the lipoplex fusion with cellular membranes facilitating the cellular uptake.<sup>14</sup>

Polyplexes are made of cationic polymers that bind DNA through electrostatic interactions between the phosphate groups present in the DNA and the cationic groups present in the polymer reagent. Polyplexes can adopt diverse nanostructures: blends, toroids, or rods, ranging from 50 to 100 nm in size.<sup>15,16</sup> Regardless of the complex topology, the size, charge, and ability to escape the lysosome and enter the nucleus appear to be the salient factors affecting transfection efficiency.<sup>17</sup>

Peptiplexes are peptide–DNA complexes that emerged over the past decade as potential gene carrier systems.<sup>18</sup> A pure peptide-based transfection agent would have several advantages over these other systems. Peptides can be more stable with regard to oxidation than lipids, are easy to synthesize on a large scale, and are relatively easy to modify with cell specific recognition ligands.<sup>19</sup> However, the mechanism of how they bind to and condense DNA is poorly documented in comparison to lipoplexes and polyplexes. Mann et al.<sup>20</sup> recently studied different patterns of DNA condensation in the presence of lysine and arginine based homopeptides and observed a correlation between different shapes of “peptiplexes” and gene delivery efficiency.<sup>21</sup>

Recently, we reported results on a set of peptides that self-assemble to form stable nanocapsules<sup>22</sup> with lipid-like properties.<sup>23</sup> The branched amphiphilic peptides capsules, termed BAPCs, are able to encapsulate, retain, and deliver (*in vitro*) a variety of solutes into cells, including the alpha-emitting actinium-225 and its radioactive daughter radionuclides.<sup>24</sup> BAPCs can adopt a range of sizes from 20 nm to several micrometers in diameter depending on assembly conditions and are capable of encapsulating various solutes within the hollow cavity defined by a pure peptide bilayer. Besides being extremely stable, they are water-soluble and simple to prepare and deliver to cells.

These amphiphilic peptide sequences were designed to mimic diacyl glycerol phospholipids in architecture and hence have a hydrophilic oligo lysine segment and two identical hydrophobic tails. The peptide capsules are prepared by mixing equimolar concentrations of two related peptides: bis(FLIVIGSII)-K-KKKK and bis(FLIVI)-K-KKKK (Figure 1). The

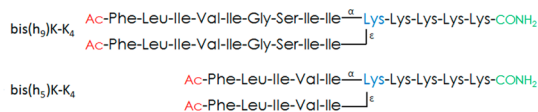


**Figure 1.** Structure of the branched amphiphilic peptides. The peptiplexes are composed of an equimolar mixture of the N-terminal acetylated bis(h<sub>9</sub>)-K-K<sub>4</sub> and bis(h<sub>5</sub>)-K-K<sub>4</sub>. The molecular weight (MW) of the peptides is 1912.29 and 1655.12, respectively.

hydrophobic core sequence is an internal fragment of the human dihydropyridine sensitive L-type calcium channel pore-forming segment, Ca<sub>v</sub>3.2.<sup>25</sup> We refer to these peptides as bis(h<sub>9</sub>)-K-K<sub>4</sub> and bis(h<sub>5</sub>)-K-K<sub>4</sub> respectively, where h<sub>9</sub> and h<sub>5</sub> refer to the number of residues within the hydrophobic segment. The mixed peptides are referred to as bis(h<sub>9</sub>:h<sub>5</sub>)-K-K<sub>4</sub>, as BAPCs when assembled into capsules in aqueous environ-

ments, and as bis(h<sub>9</sub>:h<sub>5</sub>)-K-K<sub>4</sub>-peptiplexes when associated with DNA.

Initially we hypothesized that DNA would be encapsulated during the assembly process. However, we quickly realized that assembly was disfavored in the presence of the polyanionic plasmid. We observed that, when the dried peptides are added to DNA in great molar excess, they appear to coat the polyanionic surface of dsDNA producing nanofibers. However, at low peptide concentrations we observed compaction of the DNA into nanocondensates.

In this report, we investigated the interactions of these branched amphiphilic peptides with pDNA and the ability of the resulting peptiplexes to transfect HeLa cells. Different transfection efficiencies were obtained in each case, with the compacted peptiplexes showing the highest transfection rates.

## MATERIALS AND METHODS

**Peptide Synthesis.** Peptides were synthesized as previously described.<sup>27</sup> The cleaved peptides were then washed three times with diethyl ether, dissolved in water, and then lyophilized before being stored at room temperature (rt). The peptides were purified by reversed phase HPLC and characterized using matrix-assisted laser desorption/ionization time-of-flight (MALDI TOF/TOF). The mercury containing peptides were prepared as previously described.<sup>22,26</sup>

For peptides covalently labeled with a fluorescent dye, the first amino acid coupled was N<sup>α</sup>-t-Fmoc-N<sup>ε</sup>-t-boc-L-lysine onto a 4-methylbenzhydrylamine (MBHA) resin (Anaspec Inc., Fremont, CA). After deprotection of the side chain amino group of the lysine using 80% TFA in dichloromethane chloride (DCM), the N-hydroxysuccinimide ester of the 5/6-carboxy-tetramethylrhodamine was used to couple the dye to the ε-amino site of a lysine residue in the presence of N,N-diisopropylethylamine (DIEA). The remainder of the synthesis was carried out as previously detailed.<sup>22</sup>

**Preparation of Bis(h<sub>9</sub>:h<sub>5</sub>)-K-K<sub>4</sub> Peptiplexes.** The peptides, bis(h<sub>9</sub>)-K-K<sub>4</sub> and bis(h<sub>5</sub>)-K-K<sub>4</sub>, were individually dissolved in neat 2,2,2-trifluoroethanol (TFE). Under these conditions the peptides adopt a helical conformation, thereby forcing the peptides into a monomeric state and ensuring complete mixing. Peptide concentrations were calculated using the molar absorptivity (ε) of phenylalanine in water at 257.5 nm (195 cm<sup>-1</sup> M<sup>-1</sup>). The bis(h<sub>9</sub>)-K-K<sub>4</sub> and bis(h<sub>5</sub>)-K-K<sub>4</sub> peptides were then mixed together in an equimolar ratio at final concentrations of 1.25, 2.5, 5, 10, 20, and 40 μM. The TFE was then removed under vacuum. Subsequently, 2.5 μg of the plasmid (pEGFP-N3 4.7 kb) dissolved in 1 mL of water was added dropwise to the dried peptide mixture and allowed to incubate for 10 min at room temperature before addition of CaCl<sub>2</sub> (1.0 mM final concentration). After standing for an additional 20 min, the solution was added to the cell culture. The charge ratio (N:P) between the number of primary amines (N) contained in the oligo lysine tails and the number of phosphates (P) in 2.5 μg of the 4.7 kb ds pDNA was calculated to be 0.65, 1.3, 2.6, 5.2, 10.4, and 20.8 for the 1.25, 2.5, 5, 10, 20, and 40 μM peptide concentrations, respectively. For N:P = 65.5, 50 μM final peptide concentration was used with 1 μg of pDNA in 1 mL of transfection solution.

**Confocal Laser Scanning Microscopy.** The images shown in Figures 3B,C, 7, 8, and 9 were taken using a confocal LSM 700 laser-scanning microscope (Carl Zeiss, Gottingen, Germany).

**STEM Sample Preparation.** For the scanning transmission electron microscopy (STEM) analysis the bis( $h_9$ : $h_5$ )-K-K<sub>4</sub> peptiplexes were prepared as previously described with one exception. The peptide samples were prepared in water by codissolving 0.7 molar equiv of bis( $h_9$ )-K-K<sub>4</sub> and bis( $h_5$ )-K-K<sub>4</sub> along with 0.3 molar equiv of their respective  $h_9$  and  $h_5$  cysteines adducted with Me-Hg to a final concentration of 0.1 mM. The samples were negatively stained for 10 min using a multi-isotope 2% uranyl acetate (uranium bis(acetato)-O-dioxodihydrate) (Sigma-Aldrich, St. Louis, MO) solution. The samples (6  $\mu$ L) were spotted onto grids and allowed to dry before analyzing with a FEI Tecnai F20XT field emission transmission electron microscope (FEI North America, Hillsboro, OR).

**Atomic Force Microscopy (AFM).** The plasmid DNA sample was prepared as described by Li et al.<sup>27</sup> For the peptide/DNA sample, 15  $\mu$ L volumes of Opti-MEM I 4% serum medium (Life Technologies, Grand Island, NY) containing the bis( $h_9$ : $h_5$ )-K-K<sub>4</sub> peptiplexes at an N:P ratio of 10.4 were deposited onto freshly cleaved mica substrates and incubated for 15 min at room temperature. AFM topography images of immobilized DNA and peptide samples were acquired in liquid media using the contact mode on an Innova (AFM) from Bruker, USA. The AFM scanner was calibrated using a TGZ1 silicon grating from NT-MDT, USA. We used MLCT-E cantilevers with their respective nominal spring constants of 0.1 N/m, and using set point contact forces of 1 nN or less. The AFM topography data were flattened by subtracting the background and then plotted using a second order equation incorporated in the Gwyddion analysis software.<sup>28</sup>

**Determination of Zeta Potential.** The bis( $h_9$ : $h_5$ )-K-K<sub>4</sub> peptiplexes were prepared as previously described at different charge ratios and then dissolved in a final volume of 1 mL of Opti-MEM I 4% serum medium. Zeta potentials for all dispersions were determined using a zeta-potential analyzer (Brookhaven Instruments Corporation, Holtsville, NY) equipped with a 677 nm laser. All measurements were performed in triplicate.

**Gel Electrophoresis.** The bis( $h_9$ : $h_5$ )-K-K<sub>4</sub> peptiplexes were prepared as previously described with different charge ratios and then dissolved in a final volume of 1 mL of Opti-MEM I 4% serum medium. Samples (15  $\mu$ L) of these solutions were loaded on a 0.8% agarose gel containing 0.012% ethidium bromide and run at 60 V for 40 min. After electrophoresis, the resulting DNA migration bands were visualized using a MultiDoc-it digital imaging system (Ultra-Violet Products, Upland, CA, USA).

**Plasmid Digestion with Dnase-1.** The bis( $h_9$ : $h_5$ )-K-K<sub>4</sub> peptiplexes were prepared as reported above, with 30  $\mu$ L of the bis( $h_9$ : $h_5$ )-K-K<sub>4</sub> peptiplexes dissolved in Opti-MEM I 4% serum media digested using 1  $\mu$ L of RQ-1 RNase-free Dnase-1 (Promega Corp., Madison, WI). After inactivation of the DNase, the samples were run in an agarose gel using conditions previously described.

**Cell Culture.** HeLa cells were purchased from ATCC (CCL-2) and grown in Dulbecco's modified Eagle medium DMEM (Life Technologies, Grand Island, NY) supplemented with 10% (v/v) fetal bovine serum (Life Technologies, Grand Island, NY). All cell lines were passaged by trypsinization with TrypLE Express (Life Technologies, Grand Island, NY) every third to fourth day. No antibiotics were added.

**Temperature Dependence on Cellular Uptake.** HeLa cells were seeded on 22 mm culture dishes at a density of  $1 \times 10^5$

cells per mL and grown to roughly 60% confluence. Fresh medium at 4 °C was added, and subsequently, 100  $\mu$ L of medium was replaced by a temperature controlled solution containing the bis( $h_9$ : $h_5$ )-K-K<sub>4</sub> peptiplexes prepared with 30% Rhodamine B label on the bis( $h_5$ )-K-K<sub>4</sub> peptide. Subsequently, cells were incubated for 2 h at 4 °C, then washed twice with phosphate-buffered saline (PBS) at 4 °C, and analyzed using confocal microscopy. The same cell samples were then incubated for an additional 2 h at 37 °C, washed twice with PBS at 37 °C, and then reanalyzed by confocal microscopy. For the  $\beta$ -tubulin immuno-histochemical staining, cells were fixed in 3.7% formaldehyde at rt for 2 h, followed by a wash with PBS solution containing 1% Triton-X (PBST). Subsequently, cells were incubated with anti- $\beta$ -tubulin antibody (GEnScript 2G7D4) at dilutions of 1:1000 for 6 h. After three washes with PBST, the tissues were incubated for 3 h with Alexa 488 goat anti-mouse IgG (Molecular Probes, Carlsbad, CA). Stained tissues were washed in PBST and mounted in glycerol containing 300 nM 4',6'-diamino-2-phenylindole (DAPI; 2  $\mu$ g mL<sup>-1</sup>; Sigma Chemical Co.).

**Lysosomal Colocalization of Bis( $h_9$ : $h_5$ )-K-K<sub>4</sub> Peptiplexes.** For the lysosomal immunostaining postincubation of cells with the bis( $h_9$ : $h_5$ )-K-K<sub>4</sub> peptiplexes, the cells were fixed in 3.7% paraformaldehyde (PFA) at rt for 2 h followed by washes with PBST. Subsequently, cells were incubated with mouse anti-lamp1 antibody (G1/139/5) for 1 h. The (G1/139/5) hybridoma, developed by Hauri,<sup>29</sup> was obtained from Developmental Studies Hybridoma Bank at the University of Iowa. After the incubation, cells were washed three times with PBST. Subsequently, they were incubated for 3 h with Alexa 488 labeled goat anti-mouse IgG (Molecular Probes, Carlsbad, CA). The stained tissues were washed again with PBST and mounted in glycerol containing DAPI.

**Transfection.** HeLa cells were seeded on 22 mm culture dishes at a density of  $1 \times 10^5$  cells per mL, and 24 h later at 60% confluence, all medium was removed from the wells and 800  $\mu$ L of Opti-MEM I 4% serum medium was added. Next, 200  $\mu$ L volumes of the different bis( $h_9$ : $h_5$ )-K-K<sub>4</sub> peptiplexes were added to cells and allowed to incubate in normoxic conditions for 2–6 h. After this incubation, medium and transfection reagent were removed and replaced with 1 mL of fresh DMEM containing 10% FBS in each well. The cells were returned to the incubator for 48 h. For the positive control, cells were transfected with Lipofectin (Invitrogen, Carlsbad, CA), according to the protocol supplied by the manufacturer. Some parameters were adjusted to reach optimum results in HeLa cells. Briefly, lipoplexes were formed in 200  $\mu$ L of Opti-MEM I 4% serum medium mixing 2  $\mu$ g of pDNA and 8  $\mu$ L of the transfection reagent. The lipoplexes were added to the cells and allowed to incubate for 6 h at 37 °C. Cells were then resuspended in 250  $\mu$ L of PBS containing 2% (v/v) FBS and 0.1% (v/v) propidium iodide (Life Technologies). Analyses were performed on a FACS Calibur (Becton Dickinson, Franklin Lakes, NJ, USA). The EGFP-positive/PI-negative cells were counted as positively transfected cells. The data were analyzed using ANOVA with Bonferroni post test. Also, transfection efficiency was monitored by direct counting using confocal microscopy. Experiments were performed in triplicate.

**Cell Viability Assay.** Cells were seeded on 22 mm culture dishes at a density of  $1 \times 10^5$  cells per mL and grown to roughly 60% confluence. Subsequently, 200  $\mu$ L of the medium was replaced with a medium free solution containing bis( $h_9$ : $h_5$ )-

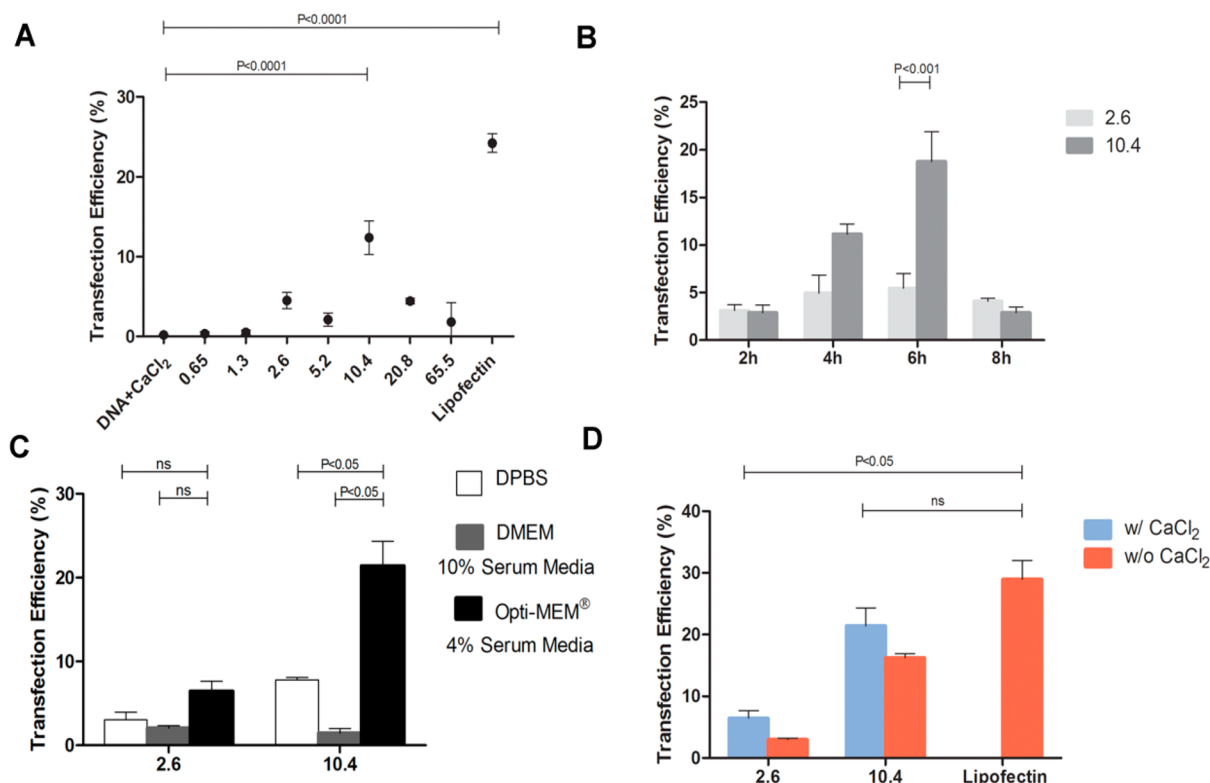


**Figure 2.** Comparison of transfection efficiency of bis( $h_9:h_5$ )-K-K<sub>4</sub> peptiplexes in HeLa cells. (A) Different peptide to DNA charge ratios (N:P) after 4 h of incubation time with the complexes in 4% serum medium and 1 mM CaCl<sub>2</sub>. (B) Different incubation times for the charge ratios 2.6 and 10.4 in 4% serum media and 1 mM CaCl<sub>2</sub>. (C) Different medium compositions used for transfection of the bis( $h_9:h_5$ )-K-K<sub>4</sub> peptiplexes, after 6 h of incubation with the complexes in 4% serum medium and 1 mM CaCl<sub>2</sub>. (D) Effect of CaCl<sub>2</sub> after 6 h of incubation time with bis( $h_9:h_5$ )-K-K<sub>4</sub> peptiplexes in 4% serum medium and 1 mM CaCl<sub>2</sub>. Data are presented as means  $\pm$  SEM (standard error of the mean). Differences between values were compared by ANOVA using Bonferroni as post test. Nonstatistical significance (ns) was considered when  $P > 0.05$ . DPBS: Dulbecco's phosphate-buffered saline, calcium and magnesium free.

K-K<sub>4</sub> peptiplexes. To check cell viability post treatment, 10  $\mu$ L volumes of the resuspended cells were mixed with 10  $\mu$ L of 2 $\times$  trypan blue solutions and allowed to sit for 2 min before being counted in a Cellometer AutoT4 automated cell counter (Nexcelom Bioscience LLC, Lawrence, MA). The data were analyzed using ANOVA with Bonferroni post test. All experiments were performed in triplicate.

## RESULTS AND DISCUSSION

**Gene Delivery and Viability Assays of Bis( $h_9:h_5$ )-K-K<sub>4</sub> Peptiplexes.** Here, we investigated the ability of bis( $h_9:h_5$ )-K-K<sub>4</sub> peptides to deliver plasmid DNA into eukaryotic cells. We hypothesized that pDNA could be trapped inside the capsules formed by the peptides even in the presence of a strong electrostatic interaction between the peptide's oligo lysyl amines and the anionic DNA backbone phosphates. Modeling studies provided an estimate of 1600–2000 peptides required for the assembly of our 20 nm diameter capsules.<sup>26–28</sup> According to this estimation, transfection experiments were carried out expecting encapsulation to occur by providing enough peptides to form one capsule/pDNA strand. The charge ratio (N:P) between the number of NH<sub>3</sub><sup>+</sup>s (N) contained in the oligo lysine tails of the peptides and the number of PO<sub>4</sub><sup>-</sup>s (P) in the 4.7 kb ds pDNA was calculated to be 65.5. This charge ratio corresponds to a 50  $\mu$ M peptide concentration or  $5 \times 10^{-8}$  mol and  $3.2 \times 10^{-7}$   $\mu$ M ds pDNA concentration or  $3.2 \times 10^{-16}$  mol for a single transfection reaction of 1 mL. These parameters were used throughout the

experiment, however, only  $\sim$ 2% of transfection efficiency was observed. This experiment was also tried using peptides composed of D-amino acids with similar results, suggesting that uptake was not dependent on cell surface binding interactions (data not shown). The observed transfection efficiency value was deemed quite low, and no more experiments were conducted using these concentrations.

Subsequently, we examined the effect of reduced peptide concentrations with a fixed pDNA concentration (N:P ratios). Surprisingly at lower N:P ratios the transfection rate in HeLa cells increased nearly 10-fold (Figure 2A). In this experiment HeLa cells were incubated for 4 h with the peptide/DNA complexes at different ratios in 4% medium. Calcium chloride (CaCl<sub>2</sub>) was added at 1 mM to improve transfection efficiency. It has been reported that adding CaCl<sub>2</sub> to cell penetrating peptides (CPP)/DNA complexes can reduce particle size and maximize gene delivery *in vitro*.<sup>30</sup> However, CaCl<sub>2</sub> by itself is capable of transfecting mammalian cells *in vitro* at certain conditions.<sup>31</sup> To account for this possibility, we studied the effect of different concentrations of CaCl<sub>2</sub> (250  $\mu$ M to 20 mM) mixed with the pDNA using HeLa cells. No GFP expression was observed with CaCl<sub>2</sub> final concentrations  $\leq$  1 mM for 6–8 h incubations. All experiments using the lower N:P ratios were conducted with and without 1 mM CaCl<sub>2</sub>.

Gene delivery efficiency was monitored qualitatively by confocal microscopy and quantified using fluorescence-activated cell sorting (FACS). Propidium iodide (PI) was used to identify and then exclude dead cells from the analysis.

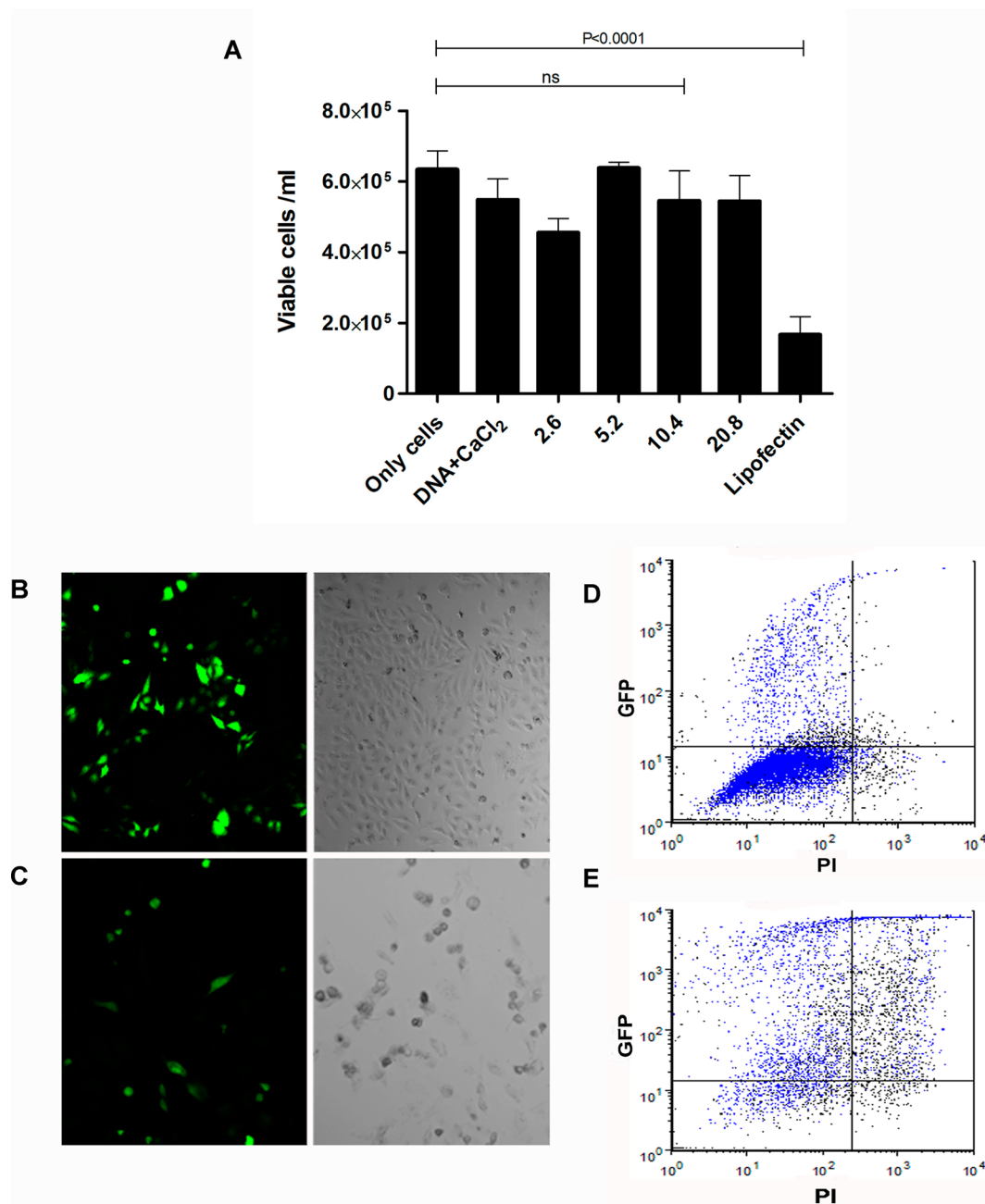


**Figure 3.** (A) Cell viability as determined by trypan blue analysis. Confocal microscopy images of HeLa cells after transfection with plasmid DNA encoding the green fluorescent protein (GFP) using (B) the peptiplex at N:P = 10.4 after 6 h of incubation in reduced serum media and 1.0 mM CaCl<sub>2</sub> and (C) Lipofectin. FACS analysis of cells transfected with the peptiplex at N:P = 10.4 (D) and the commercial reagent Lipofectin (E) using the same conditions used for the confocal studies. Data are presented as means ± SEM. The overall *P* value was determined using 1-way ANOVA using Bonferroni as post test.

The GFP-positive/PI-negative cells were counted as positively transfected cells. As a positive control, cells were transfected with the commercial transfection reagent Lipofectin using conditions optimized for this cell line.

FACS analysis showed that the N:P ratios of 2.6 and 10.4 yielded the highest gene expression with minimal toxicity. Subsequently, for these two ratios, different transfection conditions were tested to maximize gene delivery and expression.

We investigated how incubation time affects the transfection rates (Figure 2B). It was observed that a 6 h incubation with the peptide/DNA mixture produced the best transfection rate,

particularly for the ratio N:P = 10.4. Different buffers were then tested for the 2.6 and 10.4 ratios. Opti-MEM 1 4% serum medium appeared to be the most effective (Figure 2C). Figure 2D shows the effect with and without 1 mM calcium with the optimized transfection incubation time and buffer, where according to the Bonferroni post test there is no significant difference between the values from the groups 10.4 with CaCl<sub>2</sub> and Lipofectin.

It is important to note that optimal GFP expression was observed only when the plasmid was delivered in the presence of both branched peptides. The plasmid by itself, when added directly to the medium with or without 1 mM calcium, showed

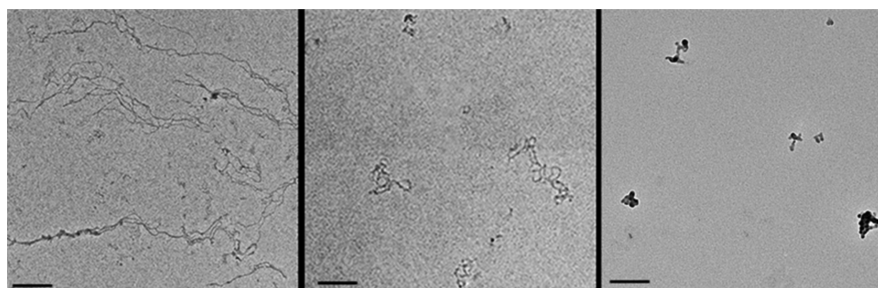
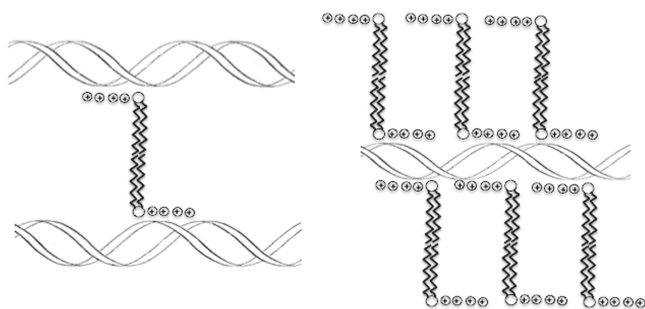


**Figure 4.** TEM images of the peptiplexes at different peptide to DNA ratios. (A) Nanofiber structures at charge ratio N:P = 65.5. (B) Plasmid DNA in the absence of peptide, shown to compare the different supramolecular structures. (C) Nanocondensate complexes formed at lower charge ratio N:P = 10.4. Scale bar = 200 nm.

### Scheme 1<sup>a</sup>



<sup>a</sup>Left panel shows a scenario in which the branched peptide sequences bridge the DNA at low N:P ratios allowing them to be pulled together. The right panel shows a hypothetical structure where the DNA is encased within a peptide bilayer. Lysines are represented by positive charges in the circles.

no GFP expression. Transfection with just one of the peptides, either bis(h<sub>9</sub>)-K-K<sub>4</sub>, bis(h<sub>5</sub>)-K-K<sub>4</sub>, or the linear sequences FLIVIGSII-K<sub>4</sub> and FLIVI-K<sub>4</sub>, showed minimal GFP expression in comparison with the bis(h<sub>9</sub>:h<sub>5</sub>)-K-K<sub>4</sub> peptiplex with the N:P ratio of 10.4 (Figure 1 in the Supporting Information). These results preclude the possibility that the transfection properties of the complex are only due to the cationic oligo lysine segment. Nevertheless, the control sequences mentioned above

are capable of condensing pDNA and facilitating translocation across the cell membrane (Figures 2A and 2B in the Supporting Information). A possible explanation of why the mixture of the two branched peptides works better than the linear sequence or just one of them could be that both peptides are required to promote the endosomal release of the peptide/DNA complex. It has been suggested for cationic lipids that incorporation of aliphatic chains with different numbers and length can improve transfection efficiency by promoting endosomal escape.<sup>32,33</sup> The alternate control peptides were tested under the same transfection conditions that yielded the highest transfection rates observed using the two different sized branched peptides.

When one considers the average ( $n = 3$ ) total number of viable cells per mL (Figure 3A) after transfecting with bis(h<sub>9</sub>:h<sub>5</sub>)-K-K<sub>4</sub>-peptiplexes at N:P 10.4 and Lipofectin, the GFP yield for the peptiplex is 1.7-fold higher than with the commercial reagent. Our results show that cell viability is minimally affected by the bis(h<sub>9</sub>:h<sub>5</sub>)-K-K<sub>4</sub>-peptiplex at the most effective N:P ratio.

Confocal analysis of living cells (Figures 3B and 3C) revealed that the cell morphology appeared normal after transfection with the peptide/DNA complexes, whereas Lipofectin treated cells appeared to have altered morphologies. The FACS analysis clearly indicated higher efficiency and minimal toxicity of the peptiplexes compared to the commercial reagent at its optimized efficiency (Figures 3D and 3E, respectively).

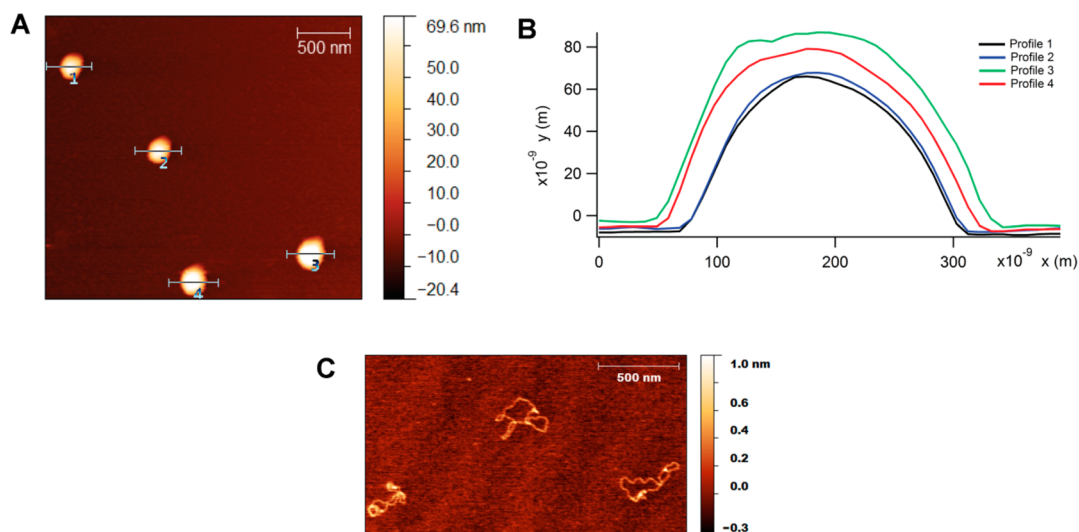


**Figure 5.** AFM images of the peptiplexes. (A)  $3 \times 2.4 \mu\text{m}$  image of the nanostructure form at N:P of 10.4. (B) Cross section analyses of the peptiplex shown in panel A. (C) Plasmid DNA alone.

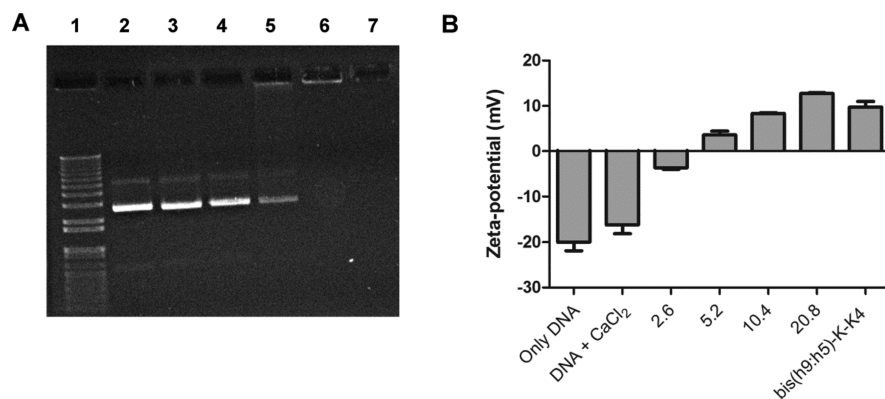


**Figure 6.** (A) Agarose gel electrophoresis of peptide complexes at different ratios; each lane contains 80 ng of pEGFP-N3. Lane 1 corresponds to 1kb dsDNA ladder. Lanes 2 and 3 contain only pEGFP-N3 plasmid in water and Opti-MEM I reduced serum medium, respectively. Lane 4 contains DNA + CaCl<sub>2</sub>, and lanes 5–7 are bis(h<sub>9</sub>:h<sub>5</sub>)-K-K<sub>4</sub> peptiplexes at 2.6, 10.4, and 20.8 respectively. (B) Zeta potential of bis(h<sub>9</sub>:h<sub>5</sub>)-K-K<sub>4</sub> peptiplexes at different peptide to DNA ratios.

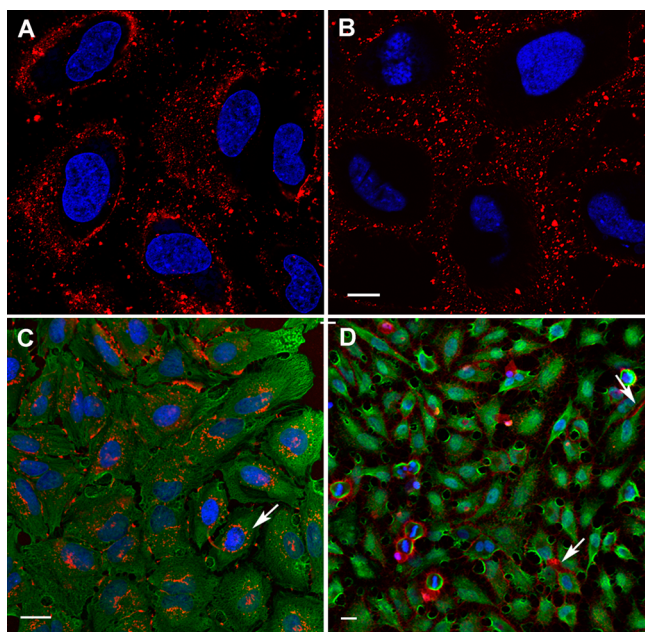


**Figure 7.** Cellular uptake of bis(h<sub>9</sub>:h<sub>5</sub>)-K-K<sub>4</sub> peptiplexes at different temperatures. The nuclei were stained with DAPI (blue), and the peptide bis(h<sub>9</sub>:h<sub>5</sub>)-K-K<sub>4</sub> was partially labeled (30%) with Rhodamine B (red). (A) Living cells showing internalization of the peptiplexes at 37 °C. (B) Living cells showing failed cellular uptake of peptiplexes at 4 °C. (C) β-Tubulin immuno-histochemical staining (green) was performed in order to assess whether the peptiplexes entered the cell at 37 °C (indicated by arrow). (D) Unsuccessful cellular uptake of peptide/DNA complexes at 4 °C showing some peptide bonded to the cell surface (indicated by arrows). Scale bar = 10 μM for upper panels and 20 μM for lower panels.

Cationic lipids containing quaternary nitrogen functional groups can bind and inhibit enzymes such as PKC, which could explain their toxicity.<sup>34</sup> In addition, cationic lipids can trigger immune responses *in vivo* and perturb the cell membrane.<sup>38</sup> Very little has been reported in regard to the toxicity of peptide carriers causing cell death.<sup>35–38</sup> Our system appears to be nontoxic for cells, suggesting that it might be safely used for *in vivo* applications.

**Biophysical Characterization of Bis(h<sub>9</sub>:h<sub>5</sub>)-K-K<sub>4</sub> Peptiplexes.** Transmission electron microscopy (TEM) of the bis(h<sub>9</sub>:h<sub>5</sub>)-K-K<sub>4</sub> peptiplexes at charge ratio of 10.4 revealed

compacted nanostructures (Figure 4A) compared to plasmid alone (Figure 4B), whereas the analysis of the ratio where we expected to see encapsulation of the DNA along the BAPCs (N:P 65.5) generated long strands of DNA. At this high peptide to DNA charge ratio the branched peptides appeared to coat the negatively charged backbone phosphate groups of the dsDNA forming nanofibers (Figure 4C).

Mann et al.<sup>24</sup> reported different patterns of DNA condensation with poly lysine and poly arginine peptides. They showed rod and sphere shaped complexes depending on the charge ratio. However, their results showed an opposite effect when compared to our results. At higher charge ratios they obtained mostly spheres whereas fibers were obtained at lower concentrations. These results suggest that our system relies on more than just electrostatic interactions.

We envision two possible mechanisms that could explain this result. At low N:P ratios the lysyl groups of monomeric branched peptides associate with the phosphates in the DNA backbone. Adjacent peptides can then associate through the hydrophobic interactions of the beta-structure hydrophobic segments thereby constraining the DNA segments in a compacted conformation. It is also conceivable that small micelle-like patches of peptides form through the association of multiple hydrophobic segments to shield themselves from water. This structure leaves the lysines solvent exposed where they are able to interact electrostatically with different portions of the DNA strands and, through bridging, stabilize the compacted DNA structure. In the case of the high N:P ratio where we see nanofibers, the peptides are in large excess over the phosphates and most likely form bilayers along the DNA surface. We know from the TEM images that the dsDNA becomes covered by the Hg-labeled peptide and that it confers protection from the nucleases tested (Figures 3 and 4 in the Supporting Information). The mercury coating was confirmed by its M-shell energy dispersive X-ray (EDX) spectra (data not shown). In water, the peptides by themselves always form a bilayer to shield the hydrophobic core residues from solvent. Therefore, we have concluded that the only logical way to coat a linear DNA sequence is to have it completely surrounded by a peptide bilayer. In this case the DNA becomes a template for the self-assembly of the peptides and becomes encased (see Scheme 1). This model suggests that by adjusting the N:P ratios different structures can be generated for the complexes. Only the high N:P ratio protected the DNA from nuclease

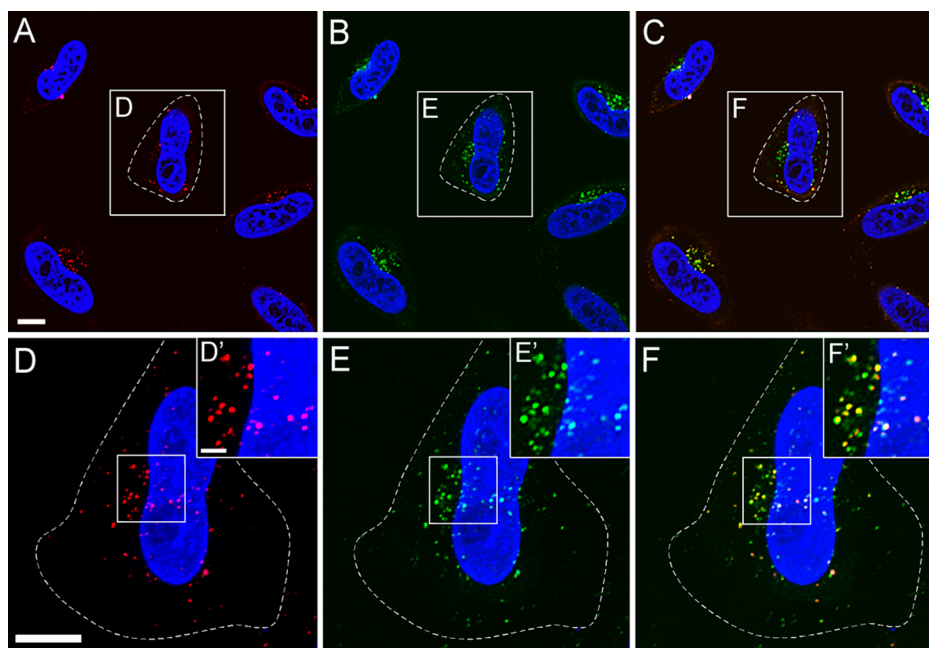


**Figure 8.** Lysosomal colocalization of bis( $h_9:h_5$ )-K-K<sub>4</sub>-peptiplexes incubated at 37 °C with 50  $\mu$ M 30% Rhodamine B label. (A) Red channel for rhodamine. (B) Green channel for lysosomal stain. (C) Merged image showing colocalization of bis( $h_9:h_5$ )-K-K<sub>4</sub>-peptiplexes and the lysosomes (yellow). D, D', E, E', F, and F' are magnifications to analyze in more detail the colocalization of the bis( $h_9:h_5$ )-K-K<sub>4</sub>-peptiplexes and the lysosomes. Scale bar, upper panel = 20  $\mu$ m, lower panel = 10  $\mu$ m.

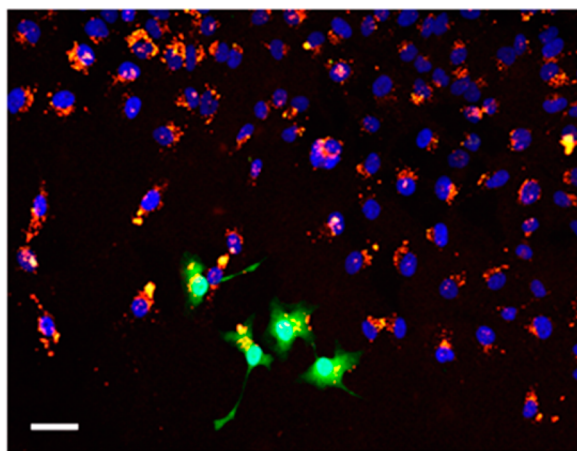


**Figure 9.** Transient EGFP expression (green) and the peptide bis( $h_9:h_5$ )-K-K<sub>4</sub> partially labeled (30%) with Rhodamine B (red) in HeLa cells visualized by confocal microscope. Yellow spots are the merge of EGFP expression and the peptide. Scale bar = 40  $\mu$ m.

cleavage. The nuclease used in this assay, DNase-1, cleaves single stranded, double stranded, and chromatin DNA and preferentially cleaves at the 5' phosphodiester linkages adjacent to pyrimidine nucleotides.<sup>39</sup>

Atomic force microscopy was used to assess the dimensions of the bis( $h_9:h_5$ )-K-K<sub>4</sub> peptiplexes using the N:P ratio of 10.4. Relatively uniform dimensions were observed for the complexes. The nanostructures displayed heights of 70–85 nm and lateral sizes of around 200–250 nm (Figures 5A and 5B). Plasmid DNA vertical height was only about 1 nm (Figure 5C). The significant change in compaction of the plasmid DNA demonstrates the peptide's ability to interact with and condense the ds pDNA.

The zeta potential of the nanostructures was also determined at the different peptide to DNA charge ratios previously tested

for transfection efficiency (Figure 6B). The surface charge for the N:P = 10.4 nanostructure that produced the highest transfection rate is +5 mV, a value suitable to facilitate interactions with negative cell membrane surfaces but not too high to cause cell damage.<sup>40,41</sup>

To further confirm the changes in charge and size of the complexes, we analyzed their electrophoretic mobility in a 0.8% agarose gel (Figure 6A). The first lane shows a 1 kb dsDNA ladder, and lanes 2 and 3 contains free pEGFP-N3 plasmid DNA in water and Opti-MEM I 4% serum medium, respectively. Lane 4 represents DNA combined with 1 mM CaCl<sub>2</sub>. For the 2.6 and 10.4 charge ratios (lanes 5 and 6) a gel shift for the complex is observed. As the peptide/DNA ratio increases, N:P = 20.8 (lane 7), the DNA is fully coated by a peptide bilayer and ethidium bromide cannot penetrate the complex, therefore DNA is not visible.

**Uptake and Cellular Colocalization of Bis( $h_9:h_5$ )-K-K<sub>4</sub> Peptiplexes.** Cellular uptake of the peptide/DNA complex that displayed the best transfection rate was monitored using confocal microscopy. For this analysis, the peptide bis( $h_9:h_5$ )-K-K<sub>4</sub> was labeled with Rhodamine B to allow visualization. To determine whether uptake of bis( $h_9:h_5$ )-K-K<sub>4</sub>-peptiplexes follows an endocytotic or nonendocytotic route, we employed the most direct and commonly used method: low temperature (4 °C) followed by return to 37 °C.<sup>42</sup> At this temperature, energy dependent endocytotic pathways are inhibited while nonendocytotic pathways are not.<sup>43</sup> Nonendocytotic uptake includes (a) membrane fusion and (b) cell penetration, which is seen in certain cationic peptides containing TAT-like and penetratin sequences that can directly penetrate the cell membrane in an energy independent manner.<sup>44,45</sup> The HeLa cells were temporarily incubated for 2 h at 4 °C with the bis( $h_9:h_5$ )-K-K<sub>4</sub>-peptiplexes at charge ratio N:P of 10.4 before being washed and imaged. The same cells were then transitioned back to 37 °C and allowed to incubate for an

additional 2 h before being reimaged. Confocal images of living cells incubated at 4 °C failed to internalize the labeled peptide/DNA complex (Figure 7A), however they appear to be associated with the cell surface. Once the cells were returned to 37 °C, normal uptake of the labeled peptide capsules was observed (Figure 7B).

Immuno-histochemical staining of  $\beta$ -tubulin was performed to confirm that the peptide/DNA complexes were inside the cells (Figures 7C and 7D). Confocal images of control cells incubated at 37 °C showed normal uptake of the labeled peptide vesicles (Figure 7C), but cells incubated at 4 °C did not show internalization of the labeled peptiplexes, only accumulation on the cell surface. These results indicate that the uptake occurs via a temperature dependent process such as endocytosis.

To examine the subcellular localization of the bis(h<sub>9</sub>:h<sub>5</sub>)-K-K<sub>4</sub>-peptiplexes after 6 h of incubation with HeLa cells, both the lysosomes (green) and peptide/pDNA complex (red) were visualized (Figure 8 panels A–D). Figure 8C shows the merged images of panels A (complexes) and B (lysosomes). A subpopulation of lysosomal markers was colocalized with the peptiplexes. These results suggest that the complexes enter the cell through the endosomal pathway yet at some point escape, most likely due to endosomal lysis. The nature of the lysosomal subpopulation has not been characterized at this time. However, regardless the exact route of entry the peptide/DNA complexes remain inside the cells without apparent degradation. In Figure 9 cells were transfected with bis(h<sub>9</sub>:h<sub>5</sub>)-K-K<sub>4</sub>-peptiplexes, and after 48 h, peptides appear to localize in the perinuclear area with EGFP expression in some of the cells.

## CONCLUSIONS

Here we report on the formulation of an alternative plasmid DNA/peptide complex that successfully transfers DNA into cultured cells with good efficiency and low cytotoxicity. As previously reported the branched peptides bis(h<sub>9</sub>:h<sub>5</sub>)-K-K<sub>4</sub>-peptides form capsules in water and act as hollow nanocarriers for small solutes.<sup>26–28</sup> In the case of large anionic molecules like nucleic acids, capsule formation is not observed. Instead, different structures are generated based on the charge ratios (N:P) between the peptides and the dsDNA. At very high charge ratios the peptides appear to coat the polyanionic surface of the dsDNA forming what appear under TEM to be long nanofibers. At low charge ratios we observed that the DNA was condensed in compacted structures within different sizes (200–300 nm). The highest transfection rate was obtained at lower ratios, 2.6 and 10.4, in the presence of 1 mM calcium chloride. Transfection efficiencies superior to that of the commercial transfection agent, Lipofectin, were observed when the total number of living transfected cells is taking into account. The simplicity of the method, low cost, and minimal cytotoxicity may make this system suitable for *in vitro* gene delivery where the transformed cells are to be clonally expanded.<sup>46</sup>

Delivery of small interfering RNAs (siRNA) into cells is a selective method to degrade mRNA (mRNA) and therefore inhibit the expression of a specific protein. siRNA therapeutics has grown rapidly, and there are several clinical trials ongoing or planned.<sup>47</sup> Another potential application could be the use of this system to deliver siRNA into diverse types of cells. The pattern of interaction of bis(h<sub>9</sub>)-K-K<sub>4</sub> and bis(h<sub>5</sub>)-K-K<sub>4</sub> with siRNA should be the same as what was observed for pDNA, fiber-type structures at high N:P ratios and compacted

structures at lower N:P ratios. Future studies will address the ability of bis(h<sub>9</sub>)-K-K<sub>4</sub> and bis(h<sub>5</sub>)-K-K<sub>4</sub> to bind and deliver siRNA into mammalian cells.

## ASSOCIATED CONTENT

### Supporting Information

Figures showing GFP expression, DNA condensation, and cellular uptake. Agarose gel showing the results of bis(h<sub>9</sub>:h<sub>5</sub>)-K-K<sub>4</sub> peptiplex samples treated with DNase-1. Figure showing N/N 1003A cells transfected with pEGFP-N3 plasmid DNA encapsulated in peptide assemblies. This material is available free of charge via the Internet at <http://pubs.acs.org>.

## AUTHOR INFORMATION

### Corresponding Author

\*141 Chalmers Hall, Department of Biochemistry, Kansas State University, Manhattan, Kansas 66506, USA. Tel: 001-785-532-5956. Fax: 001-785-532-6297. E-mail: [jtomich@ksu.edu](mailto:jtomich@ksu.edu).

### Notes

The authors declare no competing financial interest.

## ACKNOWLEDGMENTS

We acknowledge Dr. Maria Teresa Lamy and Dr. Julio H. K. Rozenfeld from the Institute of Physics, University of São Paulo, Brazil, for assisting in the zeta potential measurements. We thank Dr. Prem Thapa, from the Microscopy & Analytical Imaging Lab of University of Kansas, for help with the TEM images. Also, we thank Dr. Catherine Ewen from the flow cytometry lab of Kansas State University for her advice in analyzing flow cytometer data. This is publication 14-165-J from the Kansas Agricultural Experiment Station. Partial support for this project was provided by PHS-NIH Grant GM # R01 GM074096 (to J.M.T) and the Terry Johnson Cancer Center at Kansas State University for summer support (for P.S. and S.G.) and JSPS KAKENHI Grant # 23590649 (to T.I.).

## REFERENCES

- (1) Elsabahy, M.; Nazarali, A.; Foldvari, M. Non-viral nucleic acid delivery: key challenges and future directions. *Curr. Drug Delivery* **2011**, *8*, 235–244.
- (2) Whitehead, K. A.; Langer, R.; Anderson, D. G. Knocking down barriers: advances in siRNA delivery. *Nat. Rev. Drug Discovery* **2009**, *8*, 129–138.
- (3) Mali, P.; Esvelt, K. M.; Church, G. M. Cas9 as a versatile tool for engineering biology. *Nat. Methods* **2013**, *10*, 957–963.
- (4) Carroll, D. Genome Engineering with Zinc-Finger Nucleases. *Genetics* **2011**, *188*, 773–782.
- (5) Ray, A.; Nordén, B. Peptide nucleic acid (PNA): its medical and biotechnical applications and promise for the future. *FASEB J.* **2000**, *14*, 1041–1060.
- (6) Wu, G. Y.; Wu, C. H. Receptor-mediated gene delivery and expression *in vivo*. *J. Biol. Chem.* **1988**, *263*, 14621–14624.
- (7) Felgner, P. L.; Gadek, T. R.; Holm, M.; Roman, R.; Chan, H. W.; Wenz, M.; Northrop, J. P.; Ringold, G. M.; Danielsen, M. Lipofection: a highly efficient, lipid-mediated DNA-transfection procedure. *Proc. Natl. Acad. Sci. U.S.A.* **1987**, *84*, 7413–7417.
- (8) Pires, P.; Simoes, S.; Nir, S.; Gaspar, R.; Duzgunes, N.; Pedroso de Lima, M. C. Interaction of cationic liposomes and their DNA complexes with monocytic leukemia cells. *Biochim. Biophys. Acta* **1999**, *1418*, 71–84.
- (9) Simoes, S.; Slepishkin, V.; Pires, P.; Gaspar, R.; de Lima, M. P.; Duzgunes, N. Mechanisms of gene transfer mediated by lipoplexes associated with targeting ligands or pH-sensitive peptides. *Gene Ther.* **1999**, *6*, 1798–1807.

- (10) Wasungu, L.; Hoekstra, D. Cationic lipids, lipoplexes and intracellular delivery of genes. *J. Controlled Release* **2006**, *116*, 255–264.
- (11) Zhdanov, R. I.; Podobed, O. V.; Vlassov, V. V. Cationic lipid-DNA complexes-lipoplexes-for gene transfer and therapy. *Bioelectrochemistry* **2002**, *58*, 53–64.
- (12) Nicolau, C.; Papahadjopoulos, D. E. Liposomes and gene delivery—a perspective. In *Medical Applications of Liposomes*; Lasic, D., Papahadjopoulos, D., Eds.; Elsevier: Amsterdam, 1998; pp 347–352.
- (13) Safinya, C. R. Structures of lipid-DNA complexes: supra-molecular assembly and gene delivery. *Curr. Opin. Struct. Biol.* **2001**, *11*, 440–448.
- (14) Koynova, R.; Tenchov, T. Cationic phospholipids: structure–transfection activity relationships. *Soft Matter* **2009**, *5*, 3187–3200.
- (15) Zhou, T.; Llizo, A.; Wang, C.; Xu, G.; Yang, Y. Nanostructure-induced DNA condensation. *Nanoscale* **2013**, *5*, 8288–8306.
- (16) Fant, K.; Esbjörner, E. K.; Jenkins, A.; Gressel, M. C.; Lincoln, P.; Nordén, B. Effects of PEGylation and Acetylation of PAMAM Dendrimers on DNA Binding, Cytotoxicity and *in Vitro* Transfection Efficiency. *Mol. Pharmaceutics* **2010**, *7*, 1734–1746.
- (17) Pack, D. W.; Hoffman, A. S.; Pun, S.; Stayton, P. S. Design and development of polymers for gene delivery. *Nat. Rev. Drug Discovery* **2005**, *4*, 581–593.
- (18) Amand, H. L.; Nordén, B.; Fant, K. Functionalization with C-terminal cysteine enhances transfection efficiency of cell-penetrating peptides through dimer formation. *Biochem. Biophys. Res. Commun.* **2012**, *3*, 469–474.
- (19) Prochiantz, A. Homeoprotein Intercellular Transfer, the Hidden Face of Cell-Penetrating Peptides. In *Cell-Penetrating Peptides: Methods and Protocols*; Langel, Ü, Ed.; Springer Science+Business Media, 2011; pp 249–257.
- (20) Mann, A.; Thakur, G.; Shukla, V.; Singh, A. K.; Khanduri, R.; Naik, R.; Jiang, Y.; Kalra, N.; Dwarakanath, B. S.; Langel, U.; Ganguli, M. Differences in DNA Condensation and Release by Lysine and Arginine Homopeptides Govern Their DNA Delivery Efficiencies. *Mol. Pharmaceutics* **2011**, *8*, 1729–1741.
- (21) Branco, M. C.; Schneider, J. P. Self-assembling materials for therapeutic delivery. *Acta Biomater.* **2009**, *5*, 817–831.
- (22) Gudlur, S.; Sukthar, P.; Gao, J.; Avila, L. A.; Hiromasa, Y.; Chen, J.; Iwamoto, T.; Tomich, J. M. Peptide nanovesicles formed by the self-assembly of branched amphiphilic peptides. *PLoS One* **2012**, *7*, e45374.
- (23) Sukthar, P.; Gudlur, S.; Avila, L. A.; Whitaker, S. K.; Katz, B. B.; Hiromasa, Y.; Gao, J.; Thapa, P.; Moore, D.; Iwamoto, T.; Chen, J.; Tomich, J. M. Branched oligopeptides form nanocapsules with lipid vesicle characteristics. *Langmuir* **2013**, *29*, 14648–14654.
- (24) Sukthar, P.; Avila, L. A.; Whitaker, S. K.; Iwamoto, T.; Morgenstern, A.; Apostolidis, C.; Liu, K.; Hanzlik, R. P.; Dadachova, E.; Tomich, J. M. Branched amphiphilic peptide capsules: Cellular uptake and retention of encapsulated solutes. *Biochim. Biophys. Acta* **2014**, *1838*, 2296–2305.
- (25) Grove, A.; Tomich, J. M.; Montal, M. A molecular blueprint for the pore-forming structure of voltage gated calcium channels. *Proc. Natl. Acad. Sci. U.S.A.* **1991**, *88*, 6418–6422.
- (26) Gruen, L. C. Stoichiometry of the reaction between methylmercury(II) iodide and soluble sulphides. *Anal. Chim. Acta* **1970**, *50*, 299–303.
- (27) Li, C.; Zhao, F.; Huang, Y.; Liu, X.; Liu, Y.; Qiao, R.; Zhao, Y. Metal-free DNA linearized nuclease based on PASP-polyamine conjugates. *Bioconjugate Chem.* **2012**, *23*, 1832–1837.
- (28) Necas, D.; Klapetek, P. Gwyddion: an open-source software for SPM data analysis. *Eur. J. Phys.* **2012**, *10*, 181–188.
- (29) Schweizer, A.; Fransen, J. A.; Bachi, T.; Ginsel, L.; Hauri, H. P. Identification, by a monoclonal antibody, of a 53-kD protein associated with a tubulo-vesicular compartment at the cis-side of the Golgi apparatus. *J. Cell Biol.* **1988**, *107*, 1643–1653.
- (30) Baum, A.; Ovcharenko, D.; Berkland, C. Calcium condensed cell penetrating peptide complexes offer highly efficient, low toxicity gene silencing. *Int. J. Pharm.* **2012**, *1*, 134–42.
- (31) Kingston, R. E.; Chen, C. A.; Rose, J. K. Calcium Phosphate Transfection. *Curr. Protoc. Mol. Biol.* **2003**, *63* (9.1), 9.1.1–9.1.11 DOI: 10.1002/0471142727.mb0901s63.
- (32) Rosenzweig, H. S.; Rakhmanova, V. A.; McIntosh, T. J.; MacDonald, R. C. O-Alkyl dioleoylphosphatidylcholinium compounds: the effect of varying alkyl chain length on their physical properties and *in vitro* DNA transfection activity. *Bioconjugate Chem.* **2000**, *11*, 306–313.
- (33) Zhi, D.; Zhang, S.; Wang, B.; Zhao, Y.; Yang, B.; Yu, S. Transfection efficiency of cationic lipids with different hydrophobic domains in gene delivery. *Bioconjugate Chem.* **2010**, *21*, 563–577.
- (34) Bottega, R.; Eband, R. M. Inhibition of protein kinase C by cationic amphiphiles. *Biochemistry* **1992**, *31*, 9025–9030.
- (35) Avila, L. A.; Lee, S. Y.; Tomich, J. Synthetic *In Vitro* Delivery Systems for Plasmid DNA in Eukaryotes. *J. Nanopharmaceutics Drug Delivery* **2014**, *2*, 1–19.
- (36) Newland, B.; Zheng, Y.; Jin, Y.; Abu-Rub, M.; Cao, H.; Wang, W.; Pandit, A. Single cyclized molecule versus single branched molecule: a simple and efficient 3D “knot” polymer structure for nonviral gene delivery. *J. Am. Chem. Soc.* **2012**, *134*, 4782–4789.
- (37) Sarker, S. R.; Aoshima, Y.; Hokama, R.; Inoue, T.; Sou, K.; Takeoka, S. Arginine-based cationic liposomes for efficient *in vitro* plasmid DNA delivery with low cytotoxicity. *Int. J. Nanomed.* **2013**, *8*, 1361–1375.
- (38) Yamano, S.; Dai, J.; Yuvienco, C.; Khapli, S.; Moursi, A. M.; Montclare, J. K. Modified Tat peptide with cationic lipids enhances gene transfection efficiency via temperature-dependent and caveolae-mediated endocytosis. *J. Controlled Release* **2011**, *152*, 278–285.
- (39) Moore, S. Pancreatic DNase. In *The Enzymes*, 3rd ed.; Boyer, P. D., Ed.; Academic Press: New York, 1981; Vol. 14, pp 281–296.
- (40) Jafari, M.; Soltani, M.; Naahidi, S.; Karunarathne, D. N.; Chen, P. Nonviral approach for targeted nucleic acid delivery. *Curr. Med. Chem.* **2012**, *19*, 197–208.
- (41) Honary, S.; Zahir, F. Effect of Zeta Potential on the Properties of Nano-Drug Delivery Systems. *Trop. J. Pharm. Res.* **2013**, *2*, 265–273.
- (42) Ignatovich, I. A.; Dizhe, E. B.; Pavlotskaya, A. V.; Akifiev, B. N.; Burov, S. V.; Orlov, S. V.; Perevozchikov, A. P. Complexes of plasmid DNA with basic domain 47–57 of the HIV-1 Tat protein are transferred to mammalian cells by endocytosis-mediated pathways. *J. Biol. Chem.* **2003**, *278*, 42625–42636.
- (43) Hong, S.; Bielinska, A. U.; Mecke, A.; Keszler, B.; Beals, J. L.; Shi, X.; Balogh, L.; Orr, B. G.; Baker, J. R., Jr.; Banaszak Holl, M. M. Interaction of poly(amidoamine) dendrimers with supported lipid bilayers and cells: hole formation and the relation to transport. *Bioconjugate Chem.* **2004**, *15*, 774–782.
- (44) Gupta, B.; Levchenko, T. S.; Torchilin, V. P. Intracellular delivery of large molecules and small particles by cell-penetrating proteins and peptides. *Adv. Drug Delivery Rev.* **2005**, *57*, 637–651.
- (45) Per Thorén, E. G.; Persson, D.; Karlsson, M.; Nordén, B. The Antennapedia peptide penetrates translocates across lipid bilayers the first direct observation. *FEBS Lett.* **2000**, *482*, 265–268.
- (46) Xue, L. Y.; Chiu, S. M.; Oleinick, N. L. Atg7 deficiency increases resistance of MCF-7 human breast cancer cells to photodynamic therapy. *Autophagy* **2010**, *6*, 248–255.
- (47) Miele, E.; Spinelli, G. P.; Miele, E.; Fabrizio, E.; Ferretti, E.; Tomao, S.; Gulino, A. Nanoparticle-based delivery of small interfering RNA: challenges for cancer therapy. *Int. J. Nanomed.* **2012**, *7*, 3637–3657.